The role of MHD in the sustainment of electron internal transport barriers and H-mode in TCV

G. Turri , O. Sauter, S. Alberti, E. Asp, T.P. Goodman, L. Porte, V.S. Udintsev, C. Zucca

Ecole Polytechnique Fédérale de Lausanne (EPFL) Centre de Recherches en Physique des Plasmas, Association Euratom-Confederation Suisse CH-1015 Lausanne, Switzerland.

E-mail: Gianpaolo.Turri@epfl.ch, Olivier.Sauter@epfl.ch

Abstract. Advanced scenarios exhibit improved confinement properties, which make them attractive candidate for ITER. For these to be achieved, the sustainment of transport barriers and therefore high pressure gradients is inherent. Their stability properties both in the transient and steady state phases is a major issue [1], because of the relationship between high performances and proximity to a stability limit. Core MHD modes are one of the key issues in the development and sustainment of transport barriers, as they degrade the confinement properties and, in the worse case, disrupt the plasma. The understanding of the underlying physics can provide the means of finding regimes without modes. In TCV (Tokamak à Configuration Variable) H-mode and eITBs have been obtained with different schemes, usually accompanied by various types of MHD phenomenon [2, 3, 4]. In this paper we focus on the) low-shear Quasi-Stationary ELM free H-mode (QSEFHM) scenarios [4], which displays infrequent sawteeth and/or NTMs. In addition to that, high-performance eITBs shots are discussed, during which a variety of resistive to ideal modes ascribable to the infernal stability limit [5, 3]. Analysis of data from TCV highest performance discharges can clarify the potential threats of MHD modes in advanced scenarios. MHD core analysis of the QSEFHM [4], and of eITBs is presented, focusing on the existence of stability windows. The resulting operational stability limits are given, together with considerations regarding the projections of these results to a steady-state burning plasma.

1. Introduction

In TCV (Tokamak á Configuration Variable) the ECH (Electron Cyclotron Heating) system allows to locally modify the electron density and temperature. Due to neoclassical effects this results in the possibility to tailor the current profile. Very small and reverse magnetic shear plasma are routinely obtained, two instances of which are respectively the Quasi-Stationary ELM-Free H-Mode (QSEFHM, [4]) and high-performance eITBs (electron Internal Transport Barrier). These types of advanced scenarios, discussed in this paper, provide better confinement properties than conventional ones, mainly thanks to the reduced transport across flux surfaces, impeded by the arising of transport barriers.

The main characteristic of QSEFHM discharges is the transition to an ELM-free phase which lasts for much longer than a confinement time, once the auxiliary heating is applied. This is not accompanied by the density (and impurities) peaking often observed in non-ELMy H-Modes, drawback of the conventional ELM-free scenarios. In addition to that, the robustness

of the QSEFHM makes it a potential candidate for future exploitation, subject to further understanding and investigation of its properties.

The formation and sustainment of eITB in TCV [6] can also be accompanied by the development of MHD instabilities. The character of the observed instabilities varies from disruptive (infernal mode) to resistive (tearing mode developing magnetic island, classical or neoclassical). In addition, the MHD instabilities can cause periodic, spontaneous, slow, global oscillation of the plasma (electron temperature, density, plasma current, SXR radiation, etc). These are reminiscent of the Oscillatory Regime (O-regime [7]), which was first observed in the Tore Supra tokamak. In TCV the MHD activity and the O-regime are linked, with the first being the cause for the second [8].

MHD modes are detrimental for the confinement as they enhance perpendicular transport, and could be limiting the access to higher confinement, as possibly in the case of discharges not developing the QSEFHM. Therefore, the study of the interplay between advanced scenarios and MHD activity is of crucial importance, as well as the implementation of ways to avoid instabilities or to limit their effects.

2. The Quasi-Stationary ELM-Free H-Mode -*QSEFHM*-

In TCV H-mode are obtained with and without auxiliary electron cyclotron heating. The QSEFHM has been achieved in TCV by employing three gyrotrons at full power (1.41 MW, 118 GHz) with the vertical launcher on the third harmonic, X-polarization (X3). This regime appears to be fusion relevant because it displays good confinement properties, absence of ELMs, density and impurity peaking. Furthermore, the scenario is obtained with no momentum input,

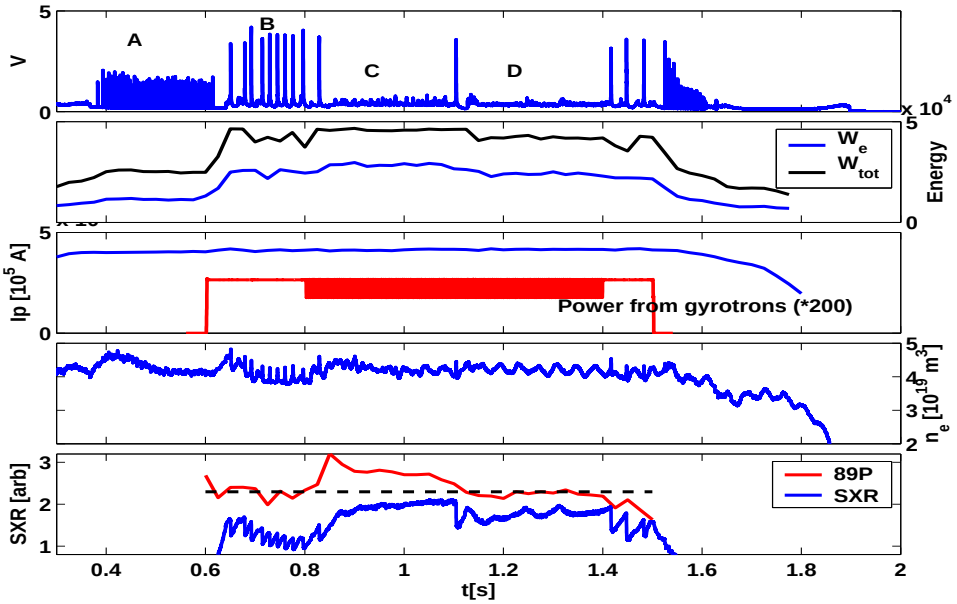

Figure 1. TCV Discharge #29892: overview of a discharge developing the quasi-stationary ELM-free H-mode. Transition A-B (top) occurs after the X3 heating is applied. At t=0.8 s, power is modulated (third plot) and soon after the plasma achieves the QSEFHM. The total and electron energy reach their maximum during the C-phase (second plot). The averaged density is almost constant (fourth plot) and the H_{98P} reaches the maximum value ~ 2.8 (bottom plot).

and in target plasmas ($\beta\sim2$, $v_{eff}\sim0.4$ and $q_{95}=2.5$) expected in ITER. Finally, TCV is in the unique position across the existing tokamaks to be able to achieve H-mode by heating solely the electrons, leaving the ions to be heated by ion-electron collisions, a scenario that mimics that

of the burning plasma [4]. The QSEFHM (figure 1) is characterized by higher-than-normal Dα baseline emission compared to the Ohmic ELMy H-mode (top plot), high energy content (second plot), high constant plasma current (third plot, corresponding to q_{95} $\sim$2.5), approximately constant electron integrated density $\bar{n}_e$ (fourth plot). The Ohmic H-mode (A) phase begins at t$\simeq$0.4 s, characterized by small and frequent ELMs. These ELMs do not display any particular MHD precursor, although sawteeth activity is present, according to SXR measurement. The sawteeth crashes and the ELMs are not coupled. The X3 [4] heating starts at t=0.6 s, which causes the transition between the phases A and B in figure 1. At this time the increase in plasma energy can be evinced from the energy trace (second plot, black trace) and the SXR emission (bottom plot, blue). The confinement scaling 98P gives H_{98P}=1.14 during this phase, and a similar value during phase D. During the B phase, the three gyrotrons are used at full power (third plot, red trace). At t=0.8 s, one of the three gyrotrons is power modulated (f=240 Hz), 30 ms before the QSEFHM begins (Dα emission, top plot). The importance (or not) of this modulation will be the subject of further experiments, as previous less resilient QSEFHM have been obtained without this feature. The ELMs become larger, and the frequency drops from 230 Hz to 60 Hz. The H_{98P} scaling gives an average value 1.4 during this phase underlying the improved confinement. The level of Dα emission (per ELM) doubles. The B-phase shows type-I ELMs, typically observed in TCV during the ECH H-mode transition. At t=0.82 s, the last ELM marks the beginning of phase-C, the quasi-stationary phase (QSEFHM). This phase does not show variation in the plasma current and averaged electron density. The plasma total energy (black trace, second plot) and electron energy (blue trace) reach their maximum value, which is kept stationary during the C-phase. At t$\simeq$1.1 s, a big ELM causes a large drop in

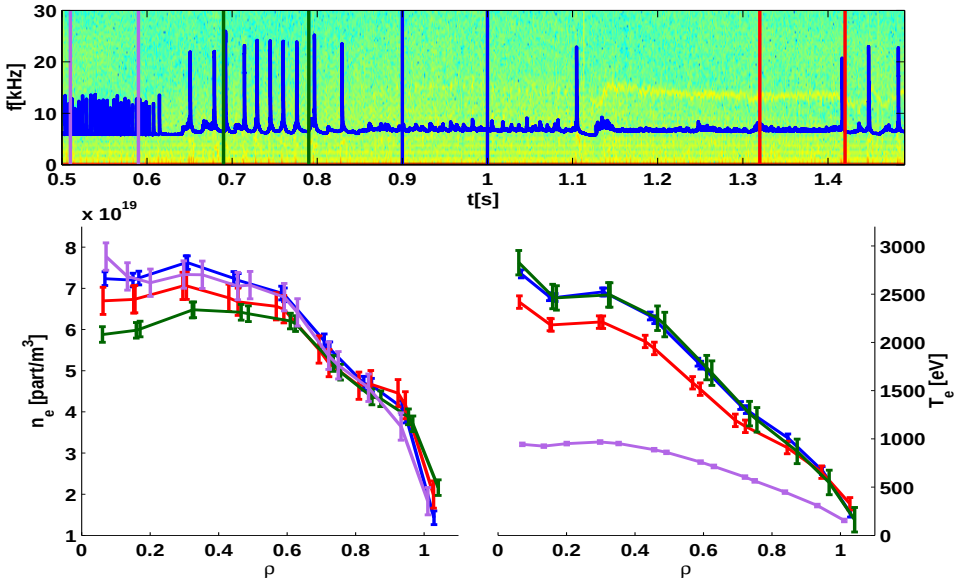

Figure 2. TCV Discharge #29892: the variation of the electron temperature and density profiles can be used to follow the different confinement properties of the four phases. The pedestal is almost constant during the H-mode, and the best confinement is achieved during the QSEFHM. The ELMy (X3) H-mode (green) and the second QSEFHM with an NTM (red) are similar in terms of confinement.

the SXR emission and energy. Conversely, the ELM does not cause any change in the averaged density. The ELM marks the transition between the first QSEFHM (C) and the second phase (D), with the latter displaying a lower energy content and H_{98P} value.

The various levels of confinement properties can be better appreciated by following the

evolution of the electron temperature and density profiles throughout the four phases of the QSEFHM discharge (figure 2). The top plot shows the spectrogram of the central soft X-ray signal (digitized at 200 kHz), with a mode whose onset is linked to the large ELM separating phase C and D (Dα trace, blue). Four time windows are chosen during the different phases, characterized by colored vertical lines. The violet profiles (electron density, bottom left; electron temperature, bottom right) represent the average Thomson Scattering (TS) profiles during the Ohmic ELMy H-mode. The density is as high as for the QSEFHM (no changes in the gas puffing are implemented during this phase), while the electron temperature is less than one third in the core. After the X3 heating is applied, the density slightly drops (-17%,larger ELMs) but the electron temperature strongly increases (green). The blue vertical lines delimit the QSEFHM; during this phase the confinement properties are the highest for both the electron temperature and density. The large ELM at t$\simeq$1.1 s triggers the NTM mode at frequency f$\sim$15 kHz, which reduces the energy (also visible in figure 1, second plot) with the temperature being lower when compared to the B-phase and the density higher. Their product is almost constant, suggesting that the effect of the NTM in the absence of ELMs is equivalent to the X3 heated, ELMy H-mode.

In the following subsection, a characterization of the MHD activity during the different phases is reported.

2.1. MHD characterization of the QSEFHM

The different phases (A to D, figure 1) show varying MHD activity, which plays an important role in defining β and H_{98P}.

- **A**: During the Ohmic ELMy H-mode, typical small sawteeth are observed. These are sometimes seen in conjunction with precursors of the m/n=1/1 type with frequency in the range 3-4 kHz; sometimes also short-lasting post-cursors are observed. The ELM activity is more rapid than the sawtooth one (f$\sim$240 Hz against f$\sim$110 Hz) and the two are decoupled. Due to the efficiency of the Ohmic heating, H_{98P} reaches the maximum during this phase.
- **B**: In the X3 heated phase the ELMs are larger and their frequency lower. The core is stabilized against the sawtooth instability, although the soft X-ray raw traces at the ELM events is similar to that observed at sawtooth crashes. The radiation profiles in this case do not show any inversion radius, instead a global collapse is observed at every ELM. Preceding and following the ELMs, a coherent m/n=2/1 oscillation is observed. This mode at f$\sim$3 kHz lasts for a few milliseconds after the crash, and it is then stabilized during the inter-ELM time, thus not having a significant impact on the confinement.
- **C**: During this phase, there is intermittent m/n=2/1 activity with $f\sim$5 kHz, which appears in bursts. Small SXR crashes are likely to be related to the m/n=2/1 mode, rather than being sawtooth crashes. This is because they appear to be linked to the mode, and the inverted SXR profiles does not suggest sawteeth activity.
- **D**: The D-phase is characterized by the single ELM event which triggers an NTM mode with $f\sim$15 kHz, and main periodicity m/n=3/2. The island full width is approximately w$\simeq$5 cm. This corresponds to an expected drop in energy of ΔW$\sim$25%, while the drop in electron energy from the reconstruction is $\sim$20% (figure 2). The resulting confinement level, from the electron energy calculations and the pressure profile from TS is comparable to that of the B-phase, i.e. that of an ELMy, X3-heated H-mode. The fact that the D-phase follows a major crash and the QSEFHM survives the presence of an NTM mode is a sign of the robustness of the scenario. The QSEFHM is therefore a viable scenario for ITER and burning plasmas. In order for it to be exploited the uncertainties regarding its attainment (in the following section a similar shot not developing the quasi-stationary regime is shown), and the potentially lethal singular ELM events require further studies.

2.2. Comparison between ELMy X3 H-mode and QSEFHM

Discharge #29894 (figure 3) was run with the same settings as discharge #29892 (QSEFHM), except for the power modulation. The pre-X3 phase for the two discharges are the same, with similar plasma current, electron density, plasma shape (l_i, k, δ). As soon as the X3 power is switched on, a large m/n=3/2 mode appears at low frequency (f≃6 kHz). This is at a time before the power modulation for #29892, hence the absence of it cannot be the cause for the mode onset. In discharge #29894 the mode rotation speeds up during the ELM-free phase lasting for approximately a confinement time (t∼50 ms), and then it slows down just before the first ELM. At the ELM event the frequency spectrum shows a steep deceleration of the mode, which is repeated for all the other ELMs (possibly suggesting a locking of the edge mode with the vessel, due to finite resistivity of the wall), all of which separated in time by approximately a confinement time. The m/n=3/2 mode is non-linearly coupled with the m/n=2/1 at f≃3

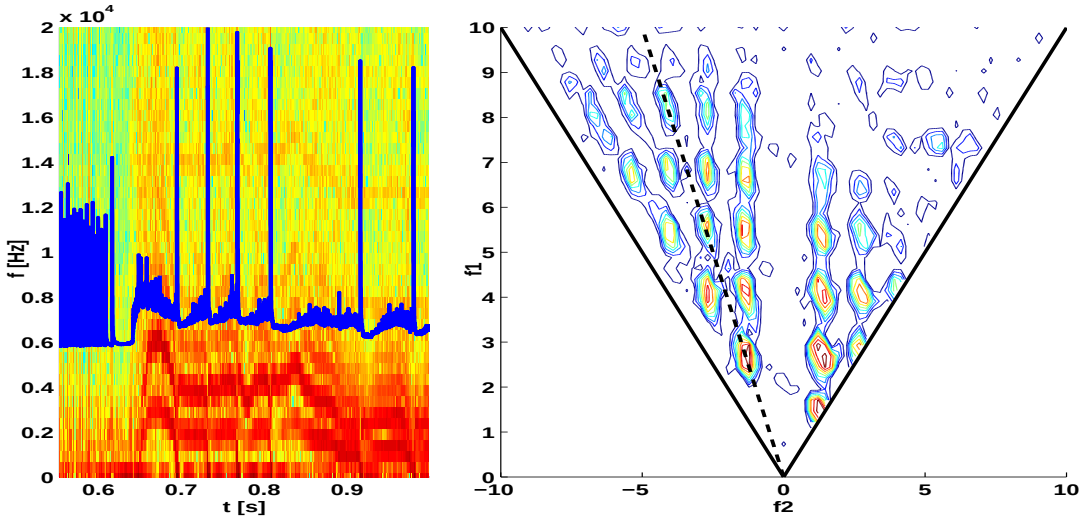

Figure 3. TCV Discharge #29894: the early MHD activity, m/n=3/2 coupled with 2/1 could prevent the access to the QSEFHM. The two modes are locked, as obtained from the bi-coherence analysis, with the 3/2 being dominant.

kHz. The mode closer to the core, i.e. the one at the q=1.5 resonant surface, is the dominant one. From a bi-coherence analysis (figure 3) the coupling (if any) of the two modes can be verified. The analysis consider the frequency relation between two coherent modes and the phase information within the Fourier transformation in the frequency space [9]. In figure 3 the correlation level between the frequencies of the two modes is approximately 0.7 at the frequency equal to the combinations of the two modes fundamental frequencies, $f1 \pm f2$. This means that the two modes are locked, i.e. they are rotating in such a way that the phase is not mixed (the phase difference between the two remains constant). The confirmation of the existence of two separate, locked modes, is also obtained through magnetic island modeling [10], where current filaments are simulated on the flux surfaces reconstructed with the LIUQE [11] code. The perturbed magnetic field is then extrapolated to the poloidal magnetic coils placed around the vessel at different poloidal locations. The result gives the degree of confidence on the mode periodicity, which is mainly m/n=3/2 with anon negligible 2/1 component. Furthermore, at a later time the lower frequency mode (m/n=2/1) is stabilized for 50 ms after an ELM, whereas the dominant 3/2 is not. Finally, the bi-coherence plot during this time interval does not show any similarities with that obtained during the times when the two modes are coexisting (figure 3).

Figure 4 shows the DMPX reconstruction of the modes, with the iso-surface of perturbed

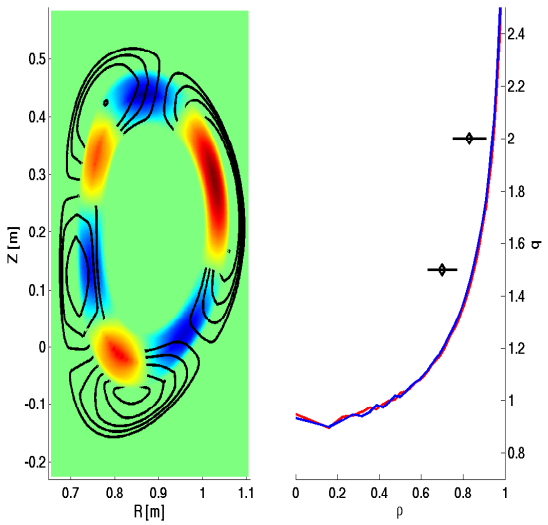

Figure 4. TCV Discharge #29894: the m/n=3/2 and 2/1 locked modes are reconstructed (left) with the high-spatial resolution SXR diagnostic. This allows to add resonance point in the q-profilie reconstruction (right).

SXR emission for the m/n=3/2 mode. The black lines represent the maximum extent of the m/n=2/1 mode, for which the interpolation returns larger error bars. Hence, these are the extremes ρ_s occupied by the external island, not its real contours. This reconstruction is useful to add resonance points on the q-reconstruction by LIUQE (figure 4). The diamond represent the best fit for the DMPX signals, and the horizontal line is an error-bar $\pm$7% of the central location, with this value chosen according to profile inversion simulation. This is useful to provide further constraints when running plasma transport simulations. The effect of the mode can be observed through the detailed comparison of the averaged TS profiles during different phases of the discharges (figure 5). **(Blue)**: during the Ohmic ELMy phase, before the development of the m/n=3/2 mode for discharge 29894, the two pressure profiles are completely overlapped (bottom-left plot), confirming that the discharges are set-up in the same way. **(Red)**: as soon as the X3 heating is commenced, discharge 29894 (second spectrogram from the top, figure 5) shows the coupled modes, together with ELMs; Discharge 29892, instead, only the ELMs and intermittent m/n=2/1 activity. The result, in terms of confined electron pressure, is an increase of the pressure for both discharges (due to the X3 heating), with discharge 29892 more than doubling the Ohmic-phase pressure, while 29894 (dashed line with diamonds) reaching a maximum that is 25% less than for 29892. This is the effect of the island (width$\simeq$7 cm), which corresponds to a loss in confinement of approximately 33% in comparison to a discharge without the mode. This is within order-of-magnitude agreement with the pressure drop between 29892 and 29894. The development of the QSEFHM is related to the available power; it is possible that the m/n=3/2 mode causing a drop in the confinement properties is reducing the probabilities to enter the quasi-stationary state. This statement requires further investigation, and further experiments are planned for the next TCV campaign. **(Green, violet)**: the variation in the confined pressure for discharge 29894 are negligible between the three phases. The mode is visible throughout the whole discharge, during X3 heating, with the frequency slowing down at t=0.9 s, and after that rotating stably at approximately f=3 kHz (m/n=3/2 mode). Although the main viable comparison is between the red phases of #29892 and #29894, another test can be done between the two discharges during the violet phase, that of the second QSEFHM for #29892. Both plasmas have a NTM-like mode, but the size and frequencies are rather different, and so are the effects on confinement. In 29892 the NTM is retained in the plasma for approximately 8

confinement times without causing a major collapse of the profiles. The plasma pressure is still 25% higher for 29892 (QSEFHM), which is the same difference observed during the X3 ELMy phase (red).

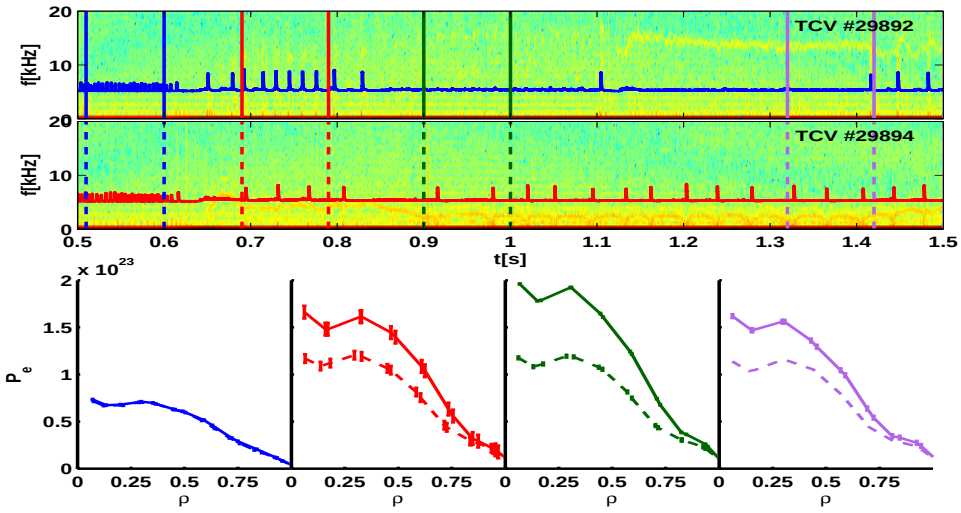

Figure 5. TCV Discharge #29894: comparison of the electron pressure profile between different phases for 29892 (QSEFHM) and 29894. The interesting phase is the X3 heated ELMy one (red), with the mode-free discharge displaying an improved confinement on the other one.

2.3. Summary on the H-mode and QSEFHM

Ohmic and ECH heated H-modes are routinely obtained on TCV, displaying type-I ELMs and other types of MHD instabilities. If X3 power is injected from the top, and the conditions in terms of plasma parameters and shape are met (together with the absence of large MHD modes) the plasma can access a quasi-stationary ELM-free H-mode (QSEFHM), with better confinement properties and absence of ELMs. The reasons for the attainment (or not) of this regime are still partly unknown, and further experiments are planned. The positive aspects are the absence of ELMs, the improved confinement, the robustness of the regime and the absence of density peaking. On the other hand, the regime cannot be easily reproduce and sometimes large ELMs are seen to interrupt the quasi-stationary phase, inducing a threat for the maximum thermal load and the possibility of triggering NTMs. MHD stability plays a fundamental role, since discharges without large magnetic islands have confinement properties up to 30% higher than discharges that develop MHD modes. In addition, no discharge has been found (up to this time) that develops the QSEFHM when the X3 heating triggers a mode on the q=1.5-2 rational surfaces before entering the quasi-stationary phase. Understanding the interplay of core MHD with the scenario achievement (if any), and the stability properties of X3 heated ELMs is a key factor for the reproducibility and safe operation of the QSEFHM. The two estimated sizes of the modes are consistent with the loss of good confinement, stressing the importance of MHD control for plasma performances.

3. Electron Internal Transport Barriers (eITBs) and the effect of MHD

Scenarios involving MHD instabilities during the flat-top of eITB are the interest of the second part of this paper. The character of the observed instabilities varies from disruptive (infernal mode) to resistive (tearing mode developing magnetic island with or without a neoclassical contribution). Figure 6 shows two eITBs experiments displaying ideal-like events: TCV

discharge #21653 and #24696. The first one (blue) reaches a very high confinement factor (H_{RLW} up to 6) thanks to the toroidal angle of injection, and the subsequent strong reverse shear. This causes a fast approach to the ideal stability limit because of the resulting current and pressure profiles. At t$\simeq$1.22 s a major disruption ideal event (ideal **infernal** mode [12]) terminates the discharge. This is shown in details on the right side of figure 6, where the time

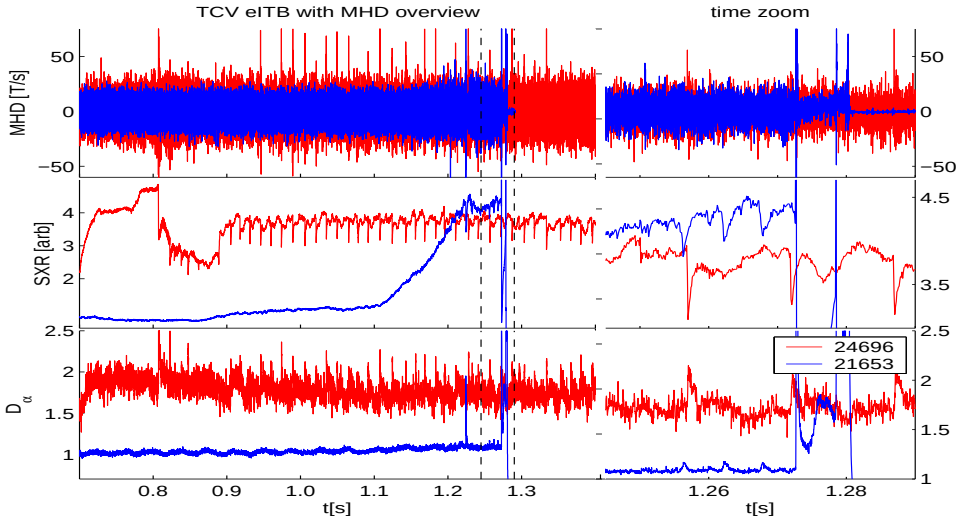

Figure 6. MHD overview for discharges #24696 (red) and #21653 (blue). From the top to the bottom: magnetic Mirnov raw signal, SXR emission from the core of the plasma, Dα emission. On the right side, zooms of the time window delimited by the vertical dashed lines.

zoom of the traces between the two vertical dashed lines is reported. The red trace, TCV

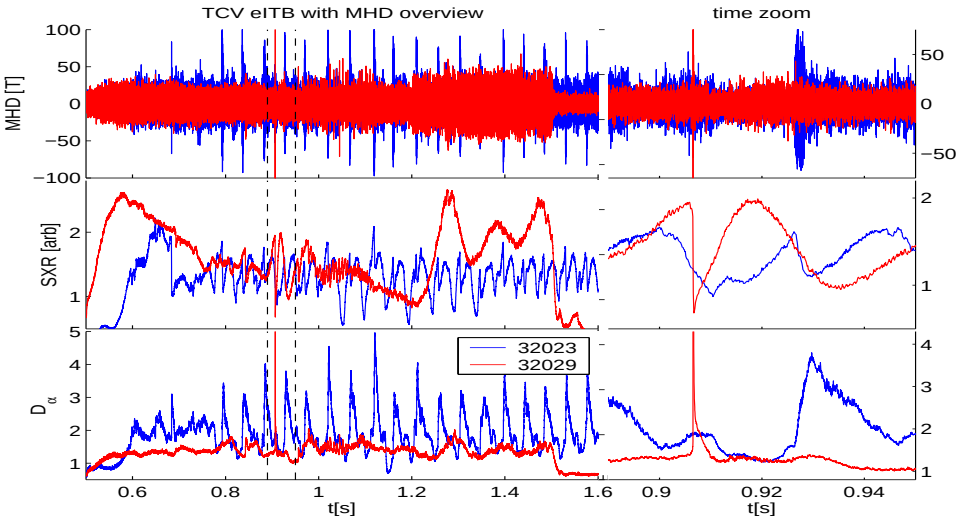

Figure 7. MHD overview for discharges #32029 (red) and #32023 (blue). From the top to the bottom: magnetic Mirnov raw signal, SXR emission from the core of the plasma, Dα emission. On the right side, zooms of the time window delimited by the vertical dashed lines.

discharge #24696, represents a different scenario involving ideal crashes with a slightly different character, called Periodical Relaxation Oscillations (PRO) in reference [13] that first described them on TCV. These ideal-like modes have the same global effect on the confinement (i.e. a

drop in the H-factor) and they resemble the β-collapse observed in JT-60U. These crashes have a *sawtooth-like* behavior of the electron temperature, with drops and subsequent rises (fig. 6, middle red trace, zoomed on the right side of the figure). It is found that each crash involves the

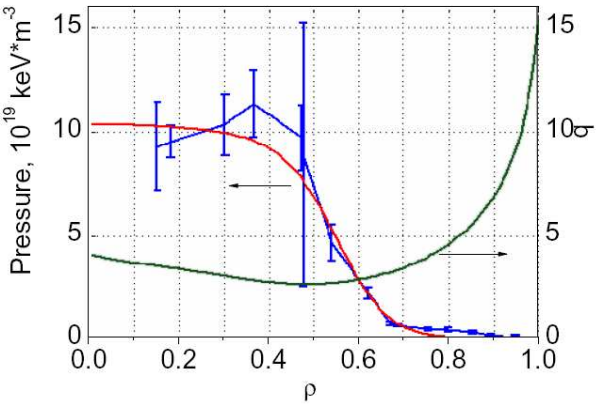

Figure 8. Thomson Scattering pressure profile from raw data (blue), with basic fit (red) and q-profile from CQL3D [14] for discharge TCV#21655. q-min$\sim$2.7 at ρ=0.5 [12].

region close to the q=2 surface, i.e. the same region involved in the presented infernal modes. This type of mode has also been previously observed in JET [15]. Regarding experiments displaying a resistive character, figure 7 shows two discharges of global plasma oscillations. The blue traces refers to discharge #32023, on-axis counter-ECCD with Ohmic contribution. The oscillations are fast and dominated by an initial ideal phase which triggers the longer lasting ($\simeq$2-5 ms) resistive phase, where the topology of the plasma is changed by the appearance of a small magnetic island. The second trace shown in figure 7 displays the emission for a fully non inductive discharge, TCV #32029 (red trace). The first phase (t$\leq$1.2 s) shows slow, huge oscillations which are terminated by ideal MHD (infernal mode). The zoom in the right part of figure 7 shows the first big crash at t$\simeq$0.92 s, which alone does not stop the oscillations. At this time the barrier is lost, but the applied heating allows the quick recreation of the barrier, and at the second time the SXR trace reaches the top, a smaller infernal mode is observed. This reduces the confinement and begins a second phase with frequent, small infernal modes (1 s$\leq$t$\leq$1.2 s), which has a detrimental effect on the confinement and prevent the development of an eITB. At a later stage, t$\geq$1.25 s, the plasma is stabilized against infernal modes and the eITB reformes, as the steep increase of SXR signal shows (red middle trace, figure 7). During the formation of the barrier, an MHD mode of resistive type appears (top trace, red, figure 7). This mode involves the periodical growth and shrink of a magnetic island located near the foot of the barrier. At the top of the oscillations the island has the minimum width and begins to increase in size, very rapidly. This reduces the confinement factor(H_{RLW} drops) until the bottom of the oscillation; at this time the island begins to shrink, the confinement improves, and the cycle starts over.

4. Description of the MHD stability during eITBs experiments

For discharge TCV #21653 (figure 6) the plasma current has been sustained by bootstrap and ECCD contribution [16]. Two gyrotrons off-axis (0.9 MW) and one gyrotron on axis (0.45 MW) were used. The non inductive current j_{CD} generated off-axis, in addition to the bootstrap current density j_{BS}, led to a hollow current density profile. The effect of the gyrotron on-axis added at t=1.1 s is evident in the middle blue trace of figure 6, with the steep increase in SXR emission [6]. The angle of injection of the on-axis launcher was varied, in order to tailor the

current profile and to change the plasma pressure profile (-15^o for #21653, -4.5^o for #21655 reported in figure 8). The current profile for discharge #21655 has been reconstructed thanks to the Fokker-Planck code CQL3D (figure 8), resulting in a q_{min} ≈2.7 at the radial location ρ_ψ ≃0.5, where the barrier is formed [12, 16]. For discharge #21653 magnetic signals analysis reveals the presence of MHD modes with periodicity m/n=3/1 and 2/1 during the disruption, with a growth time τ_{MHD} ≈20 μs, which is typical for ideal instabilities in TCV. For discharge #21655 analysis with KINX code reveals an unstable ideal infernal mode m/n=3/1 mode with a significant m/n=2/1 component, for β_N larger than 1. The β_N experimental value is close to unity, confirming that discharge #21655 is close to ideal stability threshold, with q_{min} near 3 (figure 9). The instability is caused by a high pressure gradient at ρ_ψ ≃0.5, where the eITB is formed in a low-shear region. This is the characteristic of infernal modes.

Infernal mode appears in regions of low-shear. In this region the development of low-n pressure-driven modes is possible, which was first described in [17] for reversed shear profiles. TCV plasmas are generally stable against the m/n=1/1 mode, as q_{MIN} is generally above the values for which the internal kink is unstable. Nevertheless, internal and external modes with m=2,3,4 develop when q_{MIN} is close to those integer values [12]. From the evolution of the H_{RLW}

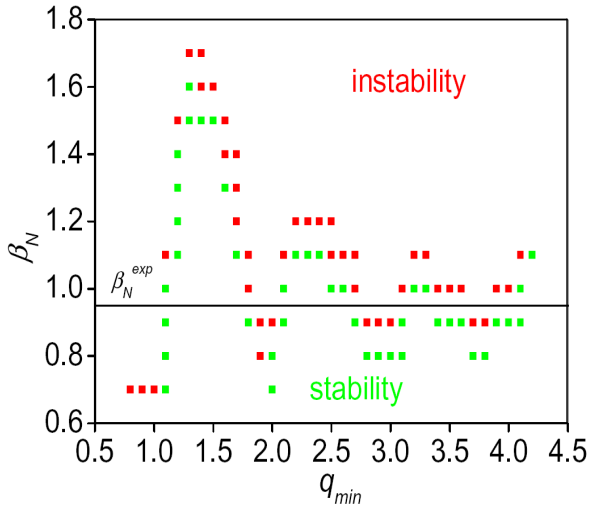

Figure 9. The n=1 mode stability boundary plotted in q_{min} space. Green and red squares correspond to ideally stable and unstable configurations respectively. β_N^{exp} is plotted for TCV discharge #21655

and the Thomson Scattering profiles, these modes are clearly detrimental for the attainment of a steady state internal transport barrier. This is a major goal for a fusion reactor, as the confinement for this regime is highly enhanced compared to that of non-advanced scenarios. A way to avoid infernal modes is to tailor the q-profile through fine adjustments of the injected power in order to move the q_{MIN} away from the minimum values of 2 and 3. For q_{min}¿4, the infernal mode becomes an external kink mode, which is less sensitive to the values of q_{min} [12].

During TCV discharge #24696 (figure 6, green trace), the gyrotrons were fired with different timing and aims compared to the previously described experiments. On-axis counter ECCD was preceded by off-axis ECH, which resulted in a broader electron temperature profile. A significant Ohmic current was also present [13]. Thus, current and pressure profiles are different from the experiments described above, and ideal periodic modes develop. These have the character of sawtooth crashes, but the inversion radius is located close to the q=2 surface. The mode is ideal kink-like and it is dominated by high local pressure gradient at the barrier location and global β limit. By combined analysis between the pressure and current profiles, the destabilizing factor

is the peaked pressure gradient in conjunction with a low shear region, which is destabilizing for the infernal modes. A fast, large crash of type m/n=2/1 at t=0.81s stops the initial fast growth of the eITB. The crash trigger a m/n=2/1 resistive mode that is stabilized later. At this time

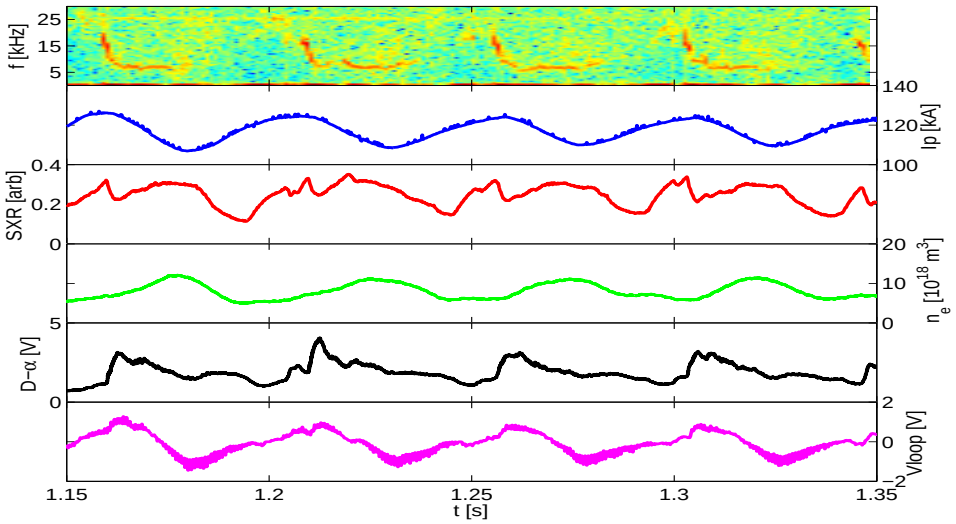

Figure 10. Overview of regular mixed ideal-type and resistive instabilities, discharge TCV #32023. From the top: magnetic spectrogram, indicating the fast ideal phase followed by a resistive mode. Plasma current (blue) which reaches the top at the onset of the infernal modes. SXR radiation from the core (red), showing the crashes at the ideal event. Plasma density (green). D-α light (black). V_{loop} (magenta) showing the continuous changes in the magnetic configuration

the confinement improves again until the pressure gradient is strong enough to trigger another infernal mode, with a period $\tau \simeq 16$ ms, which is responsible for the absence of higher H_{RLW} for this discharge. The pressure peaking factor ($p_{e0}/<p_e>$) reaches a very high value ($\simeq$15) at t=0.81 s, and this causes the relaxation of the pressure profile and a subsequent decrease in β. The following smaller crashes develop in a region with $p_{e0}/<p_e> \simeq 10$ and $\beta_N \simeq 0.75$.

If the plasma is taken further away from an ideal limit, resistive modes can be destabilized (examples are TCV #32023 and #32029). Due to the time scale of figure 7 it is not possible to appreciate the details of the MHD, which are invariably present before and during the oscillatory regime. Discharge #32023 (blue trace) is characterized by regular small infernal mode crashes with frequency $f \simeq 20$ Hz. This type of regime, with the continuous bursts of ideal activity which are followed by a longer lasting resistive mode, causes electron temperature oscillations that are triangular-like due to the ideal character.

Figure 10 shows a selection of plasma parameters evolving during four events. The spectrogram of magnetic signal (top trace) allows to appreciate the dual character of these oscillations. Every event is characterized by an ideal crash, which is responsible for the almost vertical signature indicating a large band of frequencies, from 15 kHz to 5 kHz. The ideal phase can be observed also in the SXR trace (red, third from top) and Dα light (black, 5th from top). The drop in the SXR at the occurrence of the ideal mode indicates the fast collapse of the barrier, which is generally accompanied by the emission of light. These events happen at the top of the confinement phase (highest SXR core signal), where the plasma is unstable to the infernal mode. The secondary mode is different in character and separated by the first. It is resistive and survives for $\Delta t \simeq 20$ ms. The magnetic island has a m/n=2/1 periodicity, which is also the main component of the ideal event. The plasma current (blue, second trace) shows oscillations ($\Delta I \simeq 10$kA) with the top of the plasma current synchronous with the ideal mode. The change in the current is smoother than that of SXR radiation, as these crashes are small

and the current diffusion time is much longer than the MHD time. The average density oscillates almost in phase with the SXR radiation, but with a smoother behavior. This is an indication of the different electron temperature and density dynamics. The I_p trace in particular shows that even cycles triggered by ideal modes can lead to oscillations similar to the so called *O-regime* [7]. The V_{loop} follow the general behavior of the other traces, indicating the continuous evolution of the magnetic configuration during this oscillatory regime. The drop in SXR emission during the small infernal crashes (proportional to the loss of confinement) is very limited (10% of the signal in the core). The plasma appears to shrink during the ideal mode, which probably leads to a removal of the barrier and the subsequent loss of confinement.

Discharge #32029 is unique because it shows both type of modes in a distinctive way (figure 7, 0.8 s$\leq$t$\leq$1 s for the infernal mode unstable plasma, 1.2 s$\leq$t$\leq$1.5 s for the resistive mode). At the time when the barrier is formed (t$\leq$0.8 s) the electron temperature suddenly increases (fig. 7). We can infer the beginning of an extremely large global oscillation, with a full cycle completed before an ideal instability provokes the abrupt collapse of the temperature. The radiation profiles before and after the crash show the character of a sawtooth-like instability, with an inversion radius that is located in the proximity of q=2. Based on the pressure profile and the phenomenology of the mode, the crash appears to be the result of a major infernal mode, just not large enough to disrupt the plasma as in #21653. It could be called a minor disruption or a β-collapse. In effect, it is a crash triggered by an ideal n=1 infernal mode. Another cycle begins afterwards, and this time at the top of an oscillation (t$\simeq$0.95 s) the major crash is avoided and ideal-like *burtsy* modes begin. These tinier collapses (t$\geq$0.95 s, black trace) are very frequent (Δt$\simeq$5 ms) and accompanied by MHD oscillations (f$\simeq$15 kHz); At the major crash the loss of confinement is approximately 60% of the emissions in the core. The gradients at the barrier foot are lost and expulsion of particles and heat is observed. Thanks to the applied heating and the resilience of the plasma to the crash the barrier is reformed and the cycle begins again. Later on the ideal modes are stabilized. At t=1.22 s the eITB begins to reform, which is accompanied by the development of a resistive NTM-like mode. The neoclassical character is inferred by the large bootstrap current fraction and is observed through the evolution in time of the magnetic island width. The main periodicity of the mode, obtained by concurrent analysis with Magnetic coils, Soft X-ray tomography (SXR), singular value decomposition (SVD) and Fourier analysis reveals a m/n=2/1 character. The stabilization of the ideal mode allows the formation of the eITBs, which, due to the changed plasma conditions, does not reach the highest confinement values as in the earlier stage. This, on the other hand, prevents the plasma from becoming infernal-unstable.

5. Summary on eITBs

The role of MHD stability and control is of central importance for the development of steady state eITBs in tokamak plasmas. Values of H_{RLW} higher than 4 have been obtained during eITBs discharges in TCV, with and without the development of MHD instabilities. The modes can be of ideal type (disruptions, infernal modes, PROs, ILMs) or resistive (tearing modes, NTMs), and all the intermediate states are possible. The origin of these modes is the unfavorable conjunction of large pressure gradient in a low shear region, i.e. they represent the infernal stability limit [5]. Since eITBs are essentially obtained in reverse shear plasmas and occur near q_{min}, large gradients in small shear regions are inherent of these scenarios. Therefore it is likely that the various regimes described in the literature, β-collapse, q=2 sawteeth, PRO, O-regime, minor and major disruptions in reverse shear are all related to the nearby stability limit of infernal modes. This is why they are sensitive to q_{min}, $p_0/< p >$, p' and magnetic shear [5].

The effect of all these modes is detrimental for the barrier. Avoidance of the ideal modes is necessary because of their fast growth and thus the impossibility of controlling them once developed. This can be achieved by tuning the current and heat injection, hence by changing

the current density and pressure profiles to avoid the proximity to rational integers of the safety factor 2 and 3. Regarding the resistive modes, although their effect is less abrupt, the integral effect can be as much damaging as that of the ideal mode. Favorable for these modes is the fact that they can be detected by the plasma control system, which can react in order to stabilize them, by changing the profiles or with local ECCD. Experiments with Ohmic contribution and current injection to prove this principle have been successfully achieved [2, 8].

6. Bibliography

[1] E. J. Strait. Stability of high beta tokamak plasmas@f—. *Physics of Plasmas*, 1(5):1415–1431, 1994.

[2] V.S. Udintsev and et al. Recent electron cyclotron emission results on tcv. *Fusion Science and Technology*, 52(2):161–168, August 2007.

[3] G. Turri et al. Mhd detrimental effect on the confinement during flat-top eitb plasmas on tcv. In IAEA, editor, *TM SSO Daejeon - Korea*, 2007.

[4] L. Porte et al. Plasma dynamics with second and third-harmonic ecrh and access to quasi-stationary elm-free h-mode on tcv. *Nuclear Fusion*, 47(8):952–960, 2007.

[5] J. Manickam, N. Pomphrey, and A.M.M Todd. *Nuclear Fusion*, 27:1461, 1987.

[6] T. P. Goodman et al. Safety factor profile requirements for electron itb formation in tcv. *Plasma Physics and Controlled Fusion*, 47(12B):B107–B120, 2005.

[7] G. Giruzzi, F. Imbeaux, J. L. Segui, X. Garbet, G. Huysmans, J. F. Artaud, A. Becoulet, G. T. Hoang, X. Litaudon, P. Maget, and B. Saoutic Tore Supra Team. New tokamak plasma regime with stationary temperature oscillations. *Physical Review Letters*, 91(13):135001, 2003.

[8] G. Turri et al. Mhd as trigger of plasma oscillations in eccd discharges in tcv. *Submitted to PPCF*, PPCF/259428/PAP, 2007.

[9] D Raju, O Sauter, and J B Lister. Study of nonlinear mode coupling during neoclassical tearing modes using bispectrum analysis. *Plasma Physics and Controlled Fusion*, 45(4):369–378, 2003.

[10] H. Reimerdes. *MHD Stability Limits in the TCV Tokamak*. PhD thesis, Ecole Polytechnique Fédérale de Lausanne, 2001.

[11] F. Hofmann and G. Tonetti. Tokamak equilibrium reconstruction using faraday rotation measurements. *Nuclear Fusion*, 28(10):1871–1878, 1988.

[12] A. Martynov. Ideal mhd stability of toakamk plasmas with moderate and low aspect ratio. EPFL PhD Thesis **N** 3218, (2005).

[13] G. Zhuang et al. Mhd activity in ec-heated tcv plasmas with eitbs. volume 28G, pages P–2.143, 2004.

[14] V V Parail. Energy and particle transport in plasmas with transport barriers. *Plasma Physics and Controlled Fusion*, 44(5A):A63–A85, 2002.

[15] T C Hender, P Hennequin, B Alper, T Hellsten, D F Howell, G T A Huysmans, E Joffrin, P Maget, J Manickam, M F F Nave, A Pochelon, S E Sharapov, and contributors to EFDA-JET workprogramme. Mhd stability with strongly reversed magnetic shear in jet. *Plasma Physics and Controlled Fusion*, 44(7):1143–1154, 2002.

[16] M. A. Henderson et al. Recent results from the electron cyclotron heated plasmas in tokamak [a-grave] configuration variable (tcv). *Physics of Plasmas*, 10(5):1796–1802, 2003.

[17] T. Ozeki, M. Azumi, S. Tokuda, and S. Ishida. Effects of a hollow current profile on the ideal mhd stability of high beta $_p$ plasmas in a tokamak. *Nuclear Fusion*, 33(7):1025–1035, 1993.